

Journal of Materials Chemistry A

Accepted Manuscript



This is an *Accepted Manuscript*, which has been through the Royal Society of Chemistry peer review process and has been accepted for publication.

Accepted Manuscripts are published online shortly after acceptance, before technical editing, formatting and proof reading. Using this free service, authors can make their results available to the community, in citable form, before we publish the edited article. We will replace this *Accepted Manuscript* with the edited and formatted *Advance Article* as soon as it is available.

You can find more information about *Accepted Manuscripts* in the [Information for Authors](#).

Please note that technical editing may introduce minor changes to the text and/or graphics, which may alter content. The journal's standard [Terms & Conditions](#) and the [Ethical guidelines](#) still apply. In no event shall the Royal Society of Chemistry be held responsible for any errors or omissions in this *Accepted Manuscript* or any consequences arising from the use of any information it contains.



Journal Name

COMMUNICATION

Electrochemical growth of octahedral Fe₃O₄ with high activity and stability toward oxygen reduction reaction†

Xiaofeng Zhang, Xiaoying Wang, Lijuan Le, Ai Ma and Shen Lin*

Received 00th January 20xx,
Accepted 00th January 20xx

DOI: 10.1039/x0xx00000x

www.rsc.org/

Octahedral Fe₃O₄ crystals were prepared by a facile potentiostatic deposition approach. The as-prepared Fe₃O₄ exhibits high electrocatalytic activity toward oxygen reduction reaction (ORR) and excellent stability. The unique octahedral structure provides a high density of active sites and facilitates ORR via a dominant pathway of oxygen reduction to hydroxide.

Oxygen reduction reaction has attracted great attention due to its important role in energy conversion applications including fuel cells and metal-air batteries.¹ Platinum-based materials have shown the best catalytic activity among the catalysts towards ORR. However, the high cost, scarcity, and the susceptibility to time-dependent drift of Pt catalysts seriously hinder the large-scale practical application in fuel cells.² Thus, there is an urgent demand for the development of Pt-free catalysts for ORR. In previous studies, a broad range of alternative catalysts based on nonprecious metal oxides as well as nitrogen-coordinated metal on carbon and metal-free doped carbon materials emerged.³ Among these potential materials, Fe₃O₄ can be used as a potential ORR catalyst due to its high capacity, low cost, eco-friendliness, and natural abundance. For example, Calvo et al primarily presented oxygen can be electroreduced on microporous Fe₃O₄ electrodes.⁴ Recently, graphene-supported macroporous Fe₃O₄ through hydrothermal self-assembly, freeze-drying and pyrolysis exhibited good electrocatalytic activity for the ORR in alkaline electrolyte and carbon-supported amorphous granular-like Fe₃O₄ via a solvothermal carbonization process have also been proven to be an effective ORR catalyst.⁵

Fe₃O₄ is an inverse spinel with a fcc sublattice of oxygen ions, with one third of the iron ions in valence state 2 on octahedral sites, one third in valence state 3 on octahedral sites, and one third in valence state 3 on tetrahedral sites (Fig. S1, ESI†). The high electronic conductivity in Fe₃O₄ (*ca.* $2 \times 10^4 \Omega^{-1} \text{ m}^{-1}$) is due to electron hopping by continuous electron exchange between Fe(II) and Fe(III) octahedrally coordinated positions.⁶ The ORR is assumed to take

place at octahedrally coordinated surface Fe(II).⁴ Because the ORR is a surface-structure sensitive reaction on electrodes, the exposed active sites of Fe(II) ions on the Fe₃O₄ electrocatalyst play a determinant role in the performance for the ORR. To enhance the catalytic activity for the ORR, an effective approach is to increase the exposed Fe(II) ions on Fe₃O₄ structure. In this work, the potentiostatic deposition was adopted to achieve the morphology control Fe₃O₄ structures. A new type of electrocatalyst for ORR, octahedral Fe₃O₄, can be steadily attached onto the electrode and served as an efficient catalyst for ORR in alkaline solution. To the best of our knowledge, there have been no reports of Fe₃O₄ crystals with octahedral shape as a catalyst for ORR to date. Moreover, the work on the morphology-related catalytic activity for ORR on these Fe₃O₄ remains a challenge.

The octahedral Fe₃O₄ was electrodeposited onto surface of the electrode from an alkaline solution of Fe₂(SO₄)₃ complexed with triethanol amine (TEA). The deposition was conducted at 60 °C and at a potential value of -1.1 V. The typical cyclic voltammogram (CV) is shown in Fig. 1a. The reduction begins at about -0.92 V and reaches a cathodic peak at -1.13 V. The anodic peak is located at -1.03 V. A two-step electrochemical reduction is proposed. First, the Fe(III)-TEA complex is electrochemically reduced to Fe(II) and TEA. Then the electrochemically produced Fe(II) reacts with Fe(III)-TEA in solution to produce Fe₃O₄ (Eq. S1, S2, ESI†). The *j*/*t* curve of Indium tin oxide (ITO)-coated glass substrate is shown in Fig. 1b. During the first 160 s, an increasing current is observed, corresponding to the appearance of the Fe₃O₄ crystal nucleus on

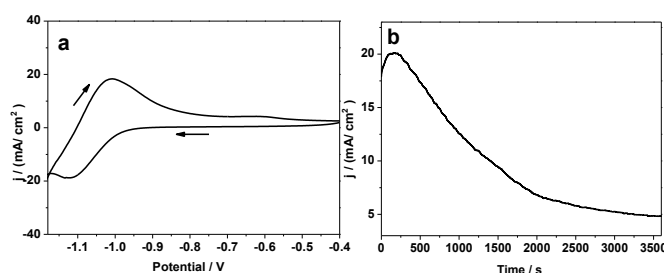


Fig. 1 (a) CV and (b) *j*-*t* curve of ITO/glass substrate in 0.09 M Fe³⁺, 0.18 M TEA and 2 M NaOH solution.

College of Chemistry and Chemical Engineering, Fujian Normal University, Fuzhou 350007, P. R. China. E-mail: shenlin@fjnu.edu.cn

† Electronic Supplementary Information (ESI) available: Experimental details, equations, some tables and figures. See DOI: 10.1039/x0xx00000x

COMMUNICATION

Journal Name

the substrate surface. When the time > 160 s, the current density decreases, corresponding to the formation of Fe_3O_4 crystals and greater surface coverage of the substrate (Fig. S2, ESI[†]).

Fig. 2(a, b) displays SEM images of the product on ITO substrate at different magnifications. The lower magnification images (Fig. 2a and Fig. S3, ESI[†]) show a large amount of octahedrons consisting of two inverted pyramids attached at their square base and bounded by eight triangular facets. The higher magnification images (Fig. 2b and Fig. S4, ESI[†]) clearly reveal that the side length of square base of octahedrons is in a range of 200–300 nm. TEM image of the Fe_3O_4 octahedrons (Fig. 2c) shows the product has a uniform tetragonal projected shape, consistent with the octahedron morphologies observed by SEM. The inset in Fig. 2c shows the HRTEM images of one typical vertexes of the octahedron. The lattice fringes give an interplanar spacing of 0.498 and 0.501 nm, which are in good agreement with the (111) and (-111) planes of Fe_3O_4 , respectively.⁷ The corresponding SAED pattern (Fig. 2d) of an individual Fe_3O_4 octahedron shows the single-crystalline nature. Based on the HRTEM image and SAED pattern, it is suggested the as-prepared Fe_3O_4 is enclosed by {111} planes, *i.e.* octahedral shape (the inset in Fig. 2d). The chemical composition of octahedral product was determined by EDS (Fig. S5, ESI[†]). In EDS spectrum, one O peak and three main Fe peaks are observed, indicating the existence of Fe and O elements in the octahedron. The molar ratio of Fe/O obtained from the result of EDS is almost 3:4, implying that the product may be Fe_3O_4 .

The XRD pattern (Fig. 3a) reveals that the electrodeposited sample is highly crystalline and can be indexed to a pure cubic spinel magnetite phase (JCPDS no.19-0629). Three elements, *i.e.* Fe, O and C, are detected in the survey XPS spectrum (Fig. S6, ESI[†]). Fig.

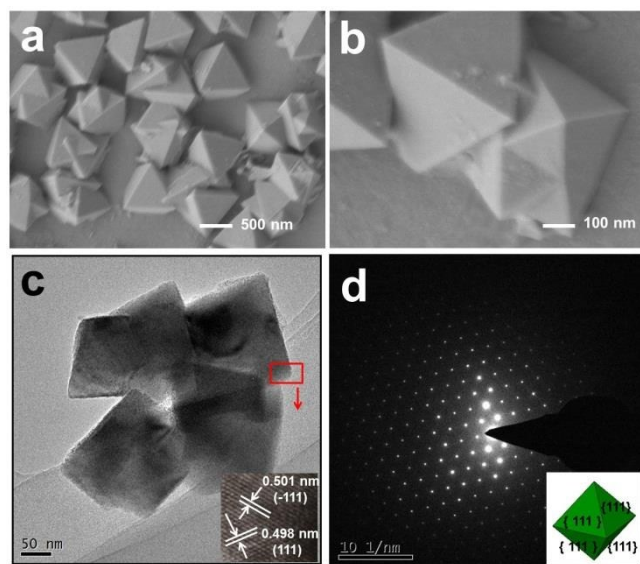


Fig. 2 (a and b) SEM images of the as-deposited product at different magnifications; (c) TEM image of the as-deposited product. The inset is HRTEM image taken from the red box areas; (d) SAED pattern of the as-deposited product and the inset is schematic model of the octahedral crystals. The products were deposited on ITO substrate.

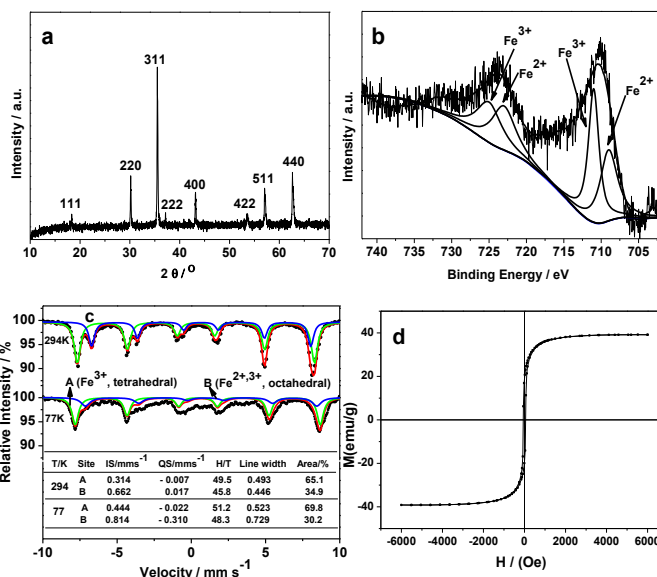


Fig. 3 (a) XRD pattern and (b) Fe 2p XPS spectra and (c) Mössbauer spectra at 294 K and 77 K and (d) hysteresis loop at 300 K of the as-deposited product. The products were deposited on ITO substrate.

3b shows the photoelectron spectrum of Fe 2p, as well as their spectral deconvolution curves. Two peaks at 710.3 and 723.9 eV are assigned to Fe 2p_{1/2} and Fe 2p_{3/2}, respectively. The absence of satellite peak at 719 eV (a major characteristic of Fe³⁺ in γ - Fe_2O_3) and 1:2 molar ratio of Fe²⁺/Fe³⁺ clearly suggests the existence of Fe_3O_4 .⁸

The Mössbauer spectra were measured at 77 K and room temperature, respectively. As shown in Fig. 3c, the hyperfine parameters are found to be in good agreement with that reported for non-stoichiometric Fe_3O_4 .⁹ Mössbauer spectra can be fitted with only two magnetically ordered components of hyperfine fields, which correspond to Fe³⁺ ions at site A and (Fe²⁺, Fe³⁺) ions at site B, respectively. The percentage of A and B could be estimated respectively based on the area of each subspectrum and the results are also similar to that of non-stoichiometric Fe_3O_4 .⁹ Fig. 3d presents the magnetic hysteresis loop of as-prepared sample. The hysteresis loop of the sample exhibits a S-shape indicating ferromagnetic behavior and the saturation magnetization obtained is ~40 emu/g, which further confirms the formation of Fe_3O_4 .¹⁰ The saturation magnetization of the Fe_3O_4 octahedron is much lower than that of Fe_3O_4 nanoparticles or the corresponding bulk materials, which may be caused by crystal anisotropy and shape anisotropy.¹¹

The electrocatalytic activity of the Fe_3O_4 deposited on glassy carbon disk electrode (GCDE) for the ORR was evaluated as compared with the commercial Pt/C catalyst. Note that the voltammetric currents of the Pt/C electrode have been normalized to electrochemically active surface areas according to the oxygen adsorption measurement method¹² and the surface area of GCDE is applied to obtain the value of current density for the Fe_3O_4 electrode. Fig. 4a shows cyclic voltammograms (CVs) of the Fe_3O_4 electrode in N₂- and O₂-saturated 0.1 M KOH at a scan rate of 50 mV s⁻¹. There is no cathodic peak from 0 to +1.2 V in N₂-saturated

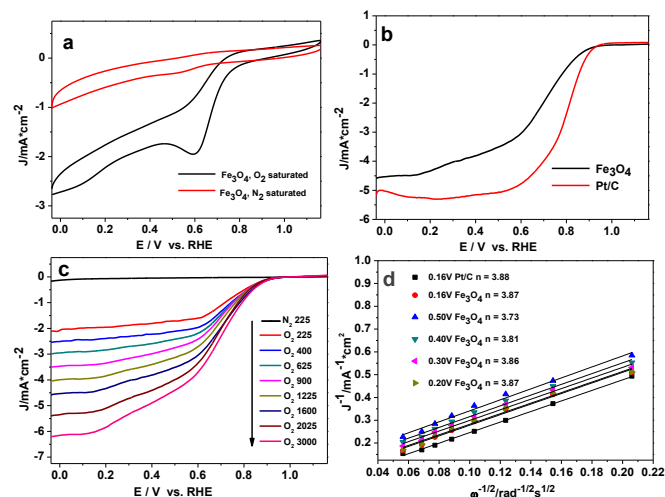


Fig. 4 (a) CVs of the electrode with as-deposited Fe_3O_4 (scan rate: 50 mV s^{-1}); (b) ORR polarization curves recorded in 0.1 M KOH saturated with O_2 at a rotating rate of 1600 rpm (scan rate: 5 mV s^{-1}); (c) ORR polarization curves of as-deposited Fe_3O_4 at different rotation rates (scan rate: 5 mV s^{-1}); (d) K-L plots for Fe_3O_4 at different potentials and Pt/C at 0.16 V . (The Fe_3O_4 and Pt/C were deposited on GCDE. The Fe_3O_4 loading was 0.6 mg cm^{-2} determined by ICP test and the Pt/C (20%) loading was $60 \mu\text{g cm}^{-2}$).

solution. When electrolyte solution was saturated with O_2 , obvious reduction currents with well-defined cathodic peak around 0.61 V appeared clearly. It indicates that O_2 can be reduced on as-deposited Fe_3O_4 . Fig. 4b displays the typical ORR polarization curves obtained at a rotation rate of 1600 rpm for Fe_3O_4 and Pt/C, respectively. ORR polarization curves of as-deposited Fe_3O_4 and Pt/C both have a sharp increase and reach saturation quickly. The ORR on Fe_3O_4 is diffusion controlled when the potential is less than 0.2 V , mixed diffusion kinetics control between 0.2 and 0.8 V and kinetics control ranging from 0.8 to 1.0 V . As can be seen in Tab. S1, kinetic currents at 0.90 V (and onsets) for octahedral Fe_3O_4 were -0.20 mA cm^{-2} (0.90 V) and -0.23 mA cm^{-2} (0.92 V) for Pt/C, indicating that as-deposited octahedral Fe_3O_4 crystals can serve as an effective catalyst for ORR. Furthermore, the as-deposited octahedral Fe_3O_4 crystals here are also compared with previously reported non-octahedral Fe_3O_4 based carbon or graphene hybrid materials: $\text{Fe}_3\text{O}_4/\text{N-C-900}^{5b}$ and $\text{Fe}_3\text{O}_4/\text{N-GAS}^{5a}$ and by recently reported Pt-alloy catalyst, PtPd/N-CNT¹³ (Tab. S1, ESI[†]). Although the onset potential of the as-deposited octahedral Fe_3O_4 (0.90 V) is lower than that of PtPd/N-CNT (1.09 V), it is higher than that of $\text{Fe}_3\text{O}_4/\text{N-C-900}$ (0.85 V) and $\text{Fe}_3\text{O}_4/\text{N-GAS}$ (0.81 V), and the kinetic current density is also higher than that of non-octahedral Fe_3O_4 catalysts, suggesting the enhancement of electrochemical activity of octahedral Fe_3O_4 crystals. Moreover, the reaction kinetics of oxygen reduction was also studied with rotating disk electrode. Fig. 4c shows a series of ORR polarization curves recorded at $\text{Fe}_3\text{O}_4/\text{GCDE}$ in 0.1 M KOH solution at different rotation rates (from 225 to 3000 rpm). There is only one stage with defined current density and the limiting current density increases with increasing rotation rate. Such ORR polarization

curves features reveal the ORR on as-deposited Fe_3O_4 may proceed via a dominant pathway facilitating O_2 to OH^- (Eq. S3, ESI[†]). Fig. 4d depicts the corresponding Koutecky–Levich (K-L) plots for the Fe_3O_4 electrode at different potentials and the Pt/C electrode at 0.16 V (vs. RHE). It can be seen that the slope of given K-L plots of as-deposited Fe_3O_4 is very close to that of Pt/C. The kinetic parameters can be analyzed with the K-L equations (Eq. S4 and 5, ESI[†]). According to Eq. S4 and 5, the number of electrons transferred can be obtained from the slope and intercept of the K-L plots, respectively. It can be seen that the slopes remain approximately constant from 0.50 to 0.20 V , showing consistent numbers of transferring electron for ORR at different electrode potentials. From the slopes of the K-L plots, the numbers (n) of electrons transferred can be calculated to be 3.8 (≈ 4) for ORR on Fe_3O_4 from 0.50 V to 0.20 V , with the value of n similar to that of Pt/C ($n=3.9$, Fig. S7, ESI[†]). This result demonstrates that the ORR on Fe_3O_4 is dominated by a near four-electron ($4e$) process and O_2 is reduced to OH^- . It is worthy of note that high ORR activities of Fe_3O_4 can probably be attributed to the following aspects: (1) the octahedral Fe_3O_4 crystals are enclosed by $\{111\}$ facets and the $\{111\}$ surface is terminated by $1/2$ monolayer of iron ions, in which the outermost $1/4$ monolayer consists of octahedral Fe^{2+} cations. It was the Fe^{2+} cations that favour the ORR in alkaline solution. (2) The increase of the number of $\{111\}$ facets would result in increasing O_2 adsorption and weakening of O-O bond, then enhancing the ORR activity.¹⁴ Hence, the obtained Fe_3O_4 octahedral structure may provide more available sites for the ORR.

The chronoamperometric curves ($i-t$, Fig. 5a and Fig. S8, ESI[†]) of as-deposited Fe_3O_4 exhibits a slow attenuation and remains 92.0% of original current after $20\,000 \text{ s}$. In contrast, Pt/C shows a gradual decrease with a current loss of approximately 57.9% after $20\,000 \text{ s}$. This result clearly suggests the durability of as-deposited Fe_3O_4 is superior to that of the Pt/C catalyst. Furthermore, after $10\,000$ cycles from 0.2 to -1.0 V , the ORR measurements show only 20 mV loss in its onset potential (Fig. S9, ESI[†]). The Fe2p XPS spectra of as-deposited Fe_3O_4 catalyst before and after $10,000$ cycles stability test are also shown in Fig. S10, ESI[†]. As illustrated in Fig. S10, the binding energy of Fe varies a little and further confirms that the Fe_3O_4 catalyst exhibits better stability for ORR. In addition, the Fe_3O_4 and Pt/C catalysts

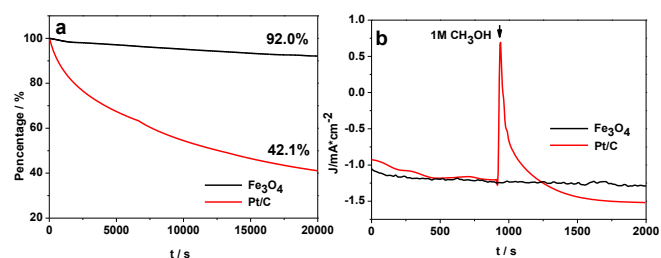


Fig. 5 (a) Chronoamperometric curves of Fe_3O_4 and Pt/C at 0.56 V (vs. RHE) in 0.1 M KOH saturated with O_2 ; (b) Chronoamperometric curves to injection of 1 M methanol into 0.1 M KOH saturated with O_2 . (The Fe_3O_4 were electrodeposited on GCDE).

were subjected to testing the possible crossover in the presence of methanol (Fig.5b). After adding methanol to the electrolyte, Fe₃O₄ keeps stable current response whereas the current responses for Pt/C catalyst instantaneously jumps to positive values owing to occurrence of methanol oxidation reaction on Pt/C.¹⁵ In order to further confirm it, the Fe₃O₄ and Pt/C catalysts have been examined by CV scans in a O₂-saturated 0.1 M KOH with 10 vol% methanol (Fig. S11, ESI[†]). No noticeable change is observed for the oxygen-reduction current at the Fe₃O₄ electrode. In contrast, Pt/C exhibits a distinct methanol oxidation reaction after the introduction of methanol, indicating that Pt/C is very sensitive to methanol crossover. This indicates that as-deposited Fe₃O₄ exhibits high selectivity for the ORR with superior ability to avoid crossover effects.

Conclusions

In this work, Fe₃O₄ crystals with octahedral shape and a size of 200-300 nm have been synthesized by a facile electrochemical deposition method. The resulting octahedral Fe₃O₄ crystals exhibit effective catalytic activities, better durability and superior methanol tolerance for ORR in alkaline solutions. The electrocatalytic performance of as-synthesized Fe₃O₄ for ORR can dominantly be attributed to their unique octahedral structure which provides a high density of Fe²⁺ active sites and facilitates ORR via a four-electron pathway. This study provides an efficient and convenient method to prepare Fe₃O₄ with octahedral structure which may serve as a potential, high effective and low-cost ORR catalyst for alkaline fuel cells.

Acknowledgements

This work was financially supported by National Natural Science Foundation of China (21171037), Natural Science Foundation of Fujian Province (2014J01033) and key item of Education Department of Fujian Province (JA13085).

Notes and references

- (a) M. K. Debe, *Nature*, 2012, **486**, 43; (b) R. Cao, J. S. Lee, M. Liu and J. Cho, *Adv. Ener. Mater.*, 2012, **2**, 816.
- (a) V. Mazumder, M. Chi, K. L. More and S. Sun, *J. Am. Chem. Soc.*, 2010, **132**, 7848; (b) S. Wang, L. Zhang, Z. Xia, A. Roy, D. W. Chang, J. B. Baek and L. Dai, *Angew. Chem. Int. Ed.*, 2012, **51**, 4209; (c) K. B. Liew, W. R. W. Daud, M. Ghasemi, J. X. Leong, S. S. Lim and M. Ismail, *Int. J. Hydrogen Energy*, 2014, **39**, 4870; (d) C. Zhu and S. Dong, *Nanoscale*, 2013, **5**, 1753.
- (a) Y. Liang, Y. Li, H. Wang, J. Zhou, J. Wang, T. Regier and H. Dai, *Nat. Mater.*, 2011, **10**, 780; (b) J. Zhang, C. Guo, L. Zhang and C. M. Li, *Chem. Commun.*, 2013, **49**, 6334; (c) X. Y. Yan, X. L. Tong, Y. F. Zhang, X. D. Han, Y. Y. Wang, G. Q. Jin, Y. Qin and X. Y. Guo, *Chem. Commun.*, 2012, **48**, 1892; (d) S. K. Kim and S. Jeon, *Electrochem. Commun.*, 2012, **22**, 141; (e) T. Kottakkat and M. Bron, *ChemElectroChem.*, 2014, **1**, 2163; (f) H. Zhu, J. Yin, X. Wang, H. Wang and X. Yang, *Adv. Funct. Mater.*, 2013, **23**, 1305; (g) S. Gao, K. Geng, H. Liu, X. Wei, M. Zhang, P. Wang and J. Wang, *Energy Environ. Sci.*, 2015, **8**, 221.
- (a) E. R. Vago and E. J. Calvo, *J. Electroanal. Chem.*, 1992, **339**, 41; (a) E. R. Vago and E. J. Calvo, *J. Chem. Soc. Faraday Trans.*, 1995, **91**, 2323; (b) E. J. Calvo, *J. Electroanal. Chem.*, 1998, **243**, 171.
- (a) Z. Wu, S. Yang, Y. Sun, K. Parvez, X. Feng and K. Müllen, *J. Am. Chem. Soc.*, 2012, **134**, 9082; (b) Y. Su, H. Jiang, Y. Zhu, X. Yang, J. Shen, W. Zou, J. Chen and C. Li, *J. Mater. Chem. A*, 2014, **2**, 7281.
- (a) E. R. Vago and E. J. Calvo, *J. Electroanal. Chem.*, 1992, **339**, 41; (b) P. A. Castro, E. R. Vago and E. J. Calvo, *J. Chem. Soc. Faraday Trans.*, 1996, **92**, 3371.
- (a) L. Zhang, J. Wu, H. Liao, Y. Hou and S. Gao, *Chem. Commun.*, 2009, **45**, 4378; (b) L. r. Meng, W. Chen, Y. Tan, L. Zou, C. Chen, H. Zhou, Q. Peng and Y. Li, *Nano Res.*, 2011, **4**, 370.
- D. Zhang, Z. Liu, S. Han, C. Li, B. Lei, M. P. Stewart, J. M. Tour and C. Zhou, *Nano Lett.*, 2004, **4**, 2151.
- A. Roychowdhury, S. P. Pati, S. Kumar and D. Das, *Powder Technol.*, 2014, **254**, 583.
- J. Wang, Q. Chen, C. Zeng and B. Hou, *Adv. Mater.*, 2004, **16**, 137.
- C. Hu, Z. Gao and X. Yang, *Chem. Phys. Lett.*, 2006, **429**, 513.
- S. Trasatti and O.A. Petrii, *Pure Appl. Chem.*, 1991, **63**, 711.
- W. J. Lee, D. S. Choi, S. H. Lee, J. Lim, J. E. Kim, D. J. Li, G. Y. Lee and S. O. Kim, *Part. Part. Syst. Charact.*, 2014, **31**, 965.
- (a) Y. Ye, J. Chen, Q. Ding, D. Lin, R. Dong, L. Yang and J. Liu, *Nanoscale*, 2013, **5**, 5887; (b) C. Lemire, R. Meyer, V. E. Henrich, Sh. Shaikhutdinov and H. J. Freund, *Surface Science*, 2004, **572**, 103; (c) E. R. Vago, E. J. Calvo, M. Stratmann, *Electrochim. Acta*, 1994, **39**, 1655.
- J. Liang, Y. Jiao, M. Jaroniec and S. Z. Qiao, *Angew. Chem. Int. Ed.*, 2012, **51**, 11496.

Octahedral Fe_3O_4 crystals was firstly examined as electrocatalyst for oxygen reduction reaction.

